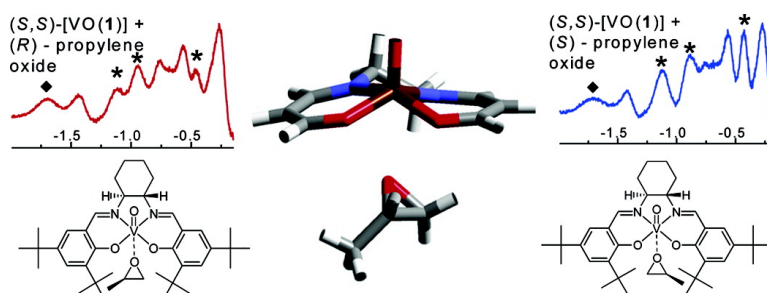


Direct Observation of Enantiomer Discrimination of Epoxides by Chiral Salen Complexes Using ENDOR

Ian A. Fallis, Damien M. Murphy, David J. Willock, Richard J. Tucker, Robert D. Farley, Robert Jenkins, and Robert R. Stevens

J. Am. Chem. Soc., **2004**, 126 (48), 15660-15661 • DOI: 10.1021/ja045491s • Publication Date (Web): 12 November 2004

Downloaded from <http://pubs.acs.org> on April 5, 2009



More About This Article

Additional resources and features associated with this article are available within the HTML version:

- Supporting Information
- Links to the 1 articles that cite this article, as of the time of this article download
- Access to high resolution figures
- Links to articles and content related to this article
- Copyright permission to reproduce figures and/or text from this article

[View the Full Text HTML](#)

Direct Observation of Enantiomer Discrimination of Epoxides by Chiral Salen Complexes Using ENDOR

Ian A. Fallis,* Damien M. Murphy,* David J. Willock, Richard J. Tucker, Robert D. Farley, Robert Jenkins, and Robert R. Strevens

School of Chemistry, Cardiff University, P.O. Box 912 Cardiff, CF10 3TB, UK

Received July 27, 2004; E-mail: fallis@cf.ac.uk; murphydm@cf.ac.uk

Enantiomer discrimination often arises from the small differences in the energies of diastereomeric states resulting from the interactions of chiral species.¹ Many analytical methods and spectroscopic techniques² can reveal the *presence* of diastereomeric interactions but do not readily yield the *spatial* arrangement of the individual chiral moieties that govern a particular diastereomeric response. As part of a study³ to investigate weak interactions of small molecules with metal complexes, we have adopted a combined ENDOR spectroscopy and computational approach to elucidate the interactions of chiral species in solution. This is made possible by analysis of the ENDOR spectra,⁴ which can often yield nuclear coordinates of the interacting species in frozen solution. Here we describe how ENDOR is used to detect weak chiral interactions between chiral paramagnetic salen complexes [VO(**1**)] and chiral epoxides (**5**) in frozen solution. We suggest that [VO(**1**)] may be a useful model for the [Co(**1**(X))]⁵ epoxide hydrolytic kinetic resolution (HKR) catalyst, developed by Jacobsen, in which a second-order rate dependence of the reaction on catalyst concentration implies activation of not only the nucleophile (water) but also of the chiral epoxide substrate.

The X-band ¹H ENDOR spectra of (*R,R*)-[VO(**1**)] in CH₂Cl₂, DMF, (*R*)-**5** and (*S*)-**5** are shown in Figure 1a–d, respectively. The ENDOR spectra of the parent [VO(**1**)] complex will first be briefly discussed before the analysis of the peaks corresponding to the coordinated epoxide moiety. A complete angular selective ENDOR analysis was carried out, but for clarity only the pure perpendicular component (field perpendicular to the V=O bond at 3290G in the EPR spectrum; Supporting Information) will be discussed. As previously reported for metal–Schiff base complexes,⁶ the proton ENDOR spectra are complex at this position; therefore, to aid in the spectral analysis, additional complexes [VO(**2**)] and [VO(**3**)] were also examined (Supporting Information). This analysis revealed that the largest ¹H hyperfine couplings in [VO(**1**)] can be systematically assigned to (i) the cyclohexyl methine (H_{lig}–VO distances of 3.05 and 3.46 Å), (ii) the imine (H_{lig}–VO distance of 4.03 Å), and (iii) the 6-*tert*-butyl protons, respectively. These distances, extracted from the simulated ENDOR data using the point–dipole approximation,^{5a–c} were confirmed using DFT calculations (3.04 and 3.48 Å for the cyclohexyl methine and 4.03 Å for the imine protons) and are in good agreement with those expected for Salen-type complexes.⁶ The DFT calculations were performed on a simplified chiral complex in which the phenyl groups in [VO(**3**)] were replaced by carbon–carbon double bonds. The extended ligand structure of [VO(**1**)] was also examined by DFT using semiempirical methods (PM3).⁷ From this, the H_{lig}–VO distances for the 6-*tert*-butyl groups of [VO(**1**)] were found to be in the range 3.38–4.05 Å due to a ~2 kJ mol⁻¹ difference in energy between rotamers. By comparison, the ENDOR spectra of [VO(**1**)] revealed an additional set of couplings that were absent

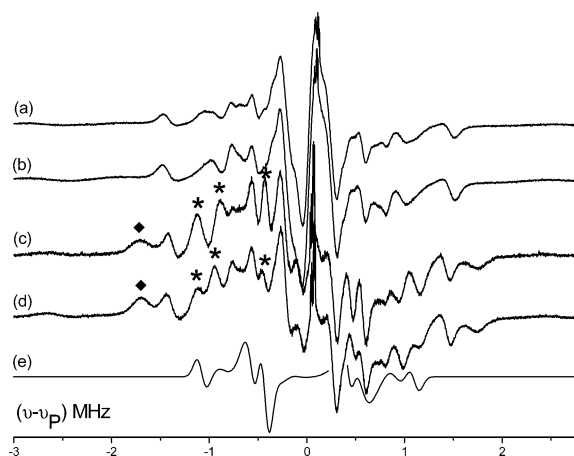
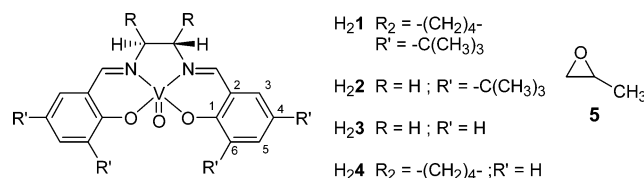


Figure 1. X-band ¹H ENDOR spectra (10 K) of (*R,R*)-[VO(**1**)] dissolved in (a) CH₂Cl₂, (b) DMF, (c) (*R*)-**5**, and (d) (*S*)-**5**; (e) simulation of epoxide peaks in spectrum d.

in [VO(**2**)], which produced a similar H_{lig}–VO distance of 3.74 Å, which we assign to all conformations of the 6-*tert*-butyl groups.



ENDOR spectra of [VO(**1**)] in noncoordinating and weakly coordinating solvents (CH₂Cl₂ and DMF, respectively, Figure 1a,b) are very similar, indicating that these solvents are not strongly bound. However, the spectrum recorded for (*R,R*)-[VO(**1**)] in (*R*)-**5** (Figure 1c) was noticeably different, with the appearance of new peaks (labeled * and ♦), which are *not* visible in the spectra of the parent complex and must arise from the coordination of the epoxide ether group to the metal center. ENDOR measurements using ²H-labeled epoxide (**5**) revealed that the * peaks originate from the epoxide, while the ♦ peak arises from a subtle conformational change in the ligand protons of [VO(**1**)]. These new peaks persist even when the solution is diluted by a factor of 10 with toluene. Coordination of the epoxide was also verified by measuring ENDOR spectra of the “diastereomeric” states, namely, (*R,R*)-[VO(**1**)] dissolved in (*S*)-**5** (Figure 1d). In this case, the pairwise combinations of (*R,R*)-[VO(**1**)] + (*R*)-**5** and (*R,R*)-[VO(**1**)] + (*S*)-**5** yield different spectra, as expected for a pair of diastereomers. Furthermore, the new peaks in Figure 1c,d possess not only different intensities but also small changes in coupling constants. This indicates that we can directly observe different *structures* for the [(*R,R*)-VO(**1**)-(*R*)-**5**] and [(*R,R*)-VO(**1**)-(*S*)-**5**] diastereomeric complexes in frozen solution.

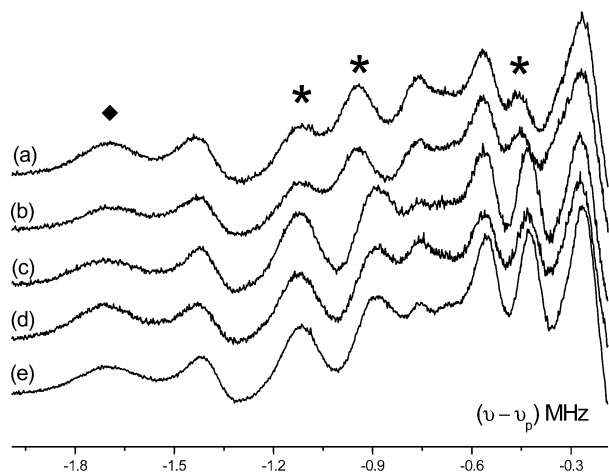


Figure 2. X-band ^1H ENDOR spectra (10 K) of the diastereomeric states formed between enantiomers of $[\text{VO}(\mathbf{1})]$ dissolved in (R) - or (S) -**5**. (a) (R,R) - $[\text{VO}(\mathbf{1})]$ in (S) -**5**, (b) (S,S) - $[\text{VO}(\mathbf{1})]$ in (R) -**5**, (c) (R,R) - $[\text{VO}(\mathbf{1})]$ in (R) -**5**, (d) (S,S) - $[\text{VO}(\mathbf{1})]$ in (S) -**5**, and (e) racemic $(R,R/S,S)$ - $[\text{VO}(\mathbf{1})]$ in racemic (R/S) -**5**.

The diastereomeric nature of these interactions was further explored by comparing all possible combinations of (R,R) -/ (S,S) - $[\text{VO}(\mathbf{1})]$ and (R) -/ (S) -**5**. Expansions of the resulting spectra are shown in Figure 2a–d. A high degree of correlation between the enantiomeric (R,R) - $[\text{VO}(\mathbf{1})]$ + (S) -**5**/ (S,S) - $[\text{VO}(\mathbf{1})]$ + (R) -**5** (Figure 2a,b) and (R,R) - $[\text{VO}(\mathbf{1})]$ + (R) -**5**/ (S,S) - $[\text{VO}(\mathbf{1})]$ + (S) -**5** (Figure 2c,d) spectra is obvious, while differences in the diastereomeric states (R,R) - $[\text{VO}(\mathbf{1})]$ + (S) -**5**/ (R,R) - $[\text{VO}(\mathbf{1})]$ + (R) -**5** (Figure 2a,c) and (S,S) - $[\text{VO}(\mathbf{1})]$ + (R) -**5**/ (S,S) - $[\text{VO}(\mathbf{1})]$ + (S) -**5** (Figure 2b,d) are notable. These results are strong evidence for the formation of diastereomeric complexes between enantiomers of $[\text{VO}(\mathbf{1})]$ and enantiomers of the weakly interacting epoxide (**5**). Furthermore, these ENDOR observations appear to be general, yielding similar enantiomeric discrimination for other aliphatic epoxides also examined (e.g., 1,2-epoxybutane, epichlorohydrin).

^1H ENDOR spectra of the racemic $[\text{VO}(\mathbf{1})]$ complex in racemic epoxide (**5**) were also recorded (Figure 2e). Significantly, this spectrum is *identical* to the spectra of the *enantiomeric* pairs (R,R) - $[\text{VO}(\mathbf{1})]$ + (R) -**5** and (S,S) - $[\text{VO}(\mathbf{1})]$ + (S) -**5**. This result represents clear, unambiguous proof for the preferential binding of (R) -**5** by (R,R) - $[\text{VO}(\mathbf{1})]$ and (S) -**5** by (S,S) - $[\text{VO}(\mathbf{1})]$. Therefore, ENDOR spectroscopy can clearly reveal that in frozen solution, one diastereomeric complex is strongly preferred.

To determine the structures of each diastereomeric complex in solution, iterative cycles of ENDOR simulation and DFT calculations were carried out. Previous ENDOR studies of vanadyl complexes have shown that coordinating solvents predominantly coordinate trans to the oxo group and in the case of $[\text{VO}(\mathbf{1})]$ it is a reasonable assumption that epoxides coordinate in a similar manner. Simulation of the peaks labeled * in Figure 1c,d and analysis of the resulting hyperfine tensors yielded two $\text{V}\cdots\text{H}_{\text{epoxide}}$ distances of 3.72 and 3.56 Å for (R,R) - $[\text{VO}(\mathbf{1})]$ in (R) -**5** and 3.76 and 3.66 Å for (R,R) - $[\text{VO}(\mathbf{1})]$ in (S) -**5** for the pair of vicinal protons on the epoxide. Essentially identical data are obtained for a similar treatment of (S,S) - $[\text{VO}(\mathbf{1})]$ + (S) -**5** and (S,S) - $[\text{VO}(\mathbf{1})]$ + (R) -**5**, respectively. It is important to note that the EPR spectra of diastereomeric combinations of $[\text{VO}(\mathbf{1})]$ and **5** are identical, regardless of the enantiomeric composition of the reaction mixture (Supporting Information). Thus, we need to use ENDOR's ability to resolve the weak electron–nuclear interactions in order to reveal the subtle structural differences between diastereomeric species.

While ENDOR is useful for determining $\text{VO}\cdots\text{H}_{\text{epoxide}}$ distances,

the $\text{VO}\cdots\text{O}_{\text{epoxide}}$ distance must be obtained by an alternative method. Thus, DFT calculations at the B3LYP/6-31G(d) function⁷ using the earlier model yielded epoxide adducts in which the $\text{VO}\cdots\text{O}_{\text{epoxide}}$ distances were calculated as 2.81 and 2.85 Å for (R,R) - $[\text{VO}(\mathbf{1})]$ + (S) -**5** and (R,R) - $[\text{VO}(\mathbf{1})]$ + (R) -**5**, respectively. Although these distances are long, they can be rationalized by considering the known pyramidalization at V in $[\text{VO}(\mathbf{1}-3)]$ -type complexes, which renders the metal center less accessible to donor groups,^{4b} and the poor donor ability of epoxides, as evidenced by the paucity of structurally characterized metal–epoxide complexes. Additionally, the corresponding $\text{VO}\cdots\text{H}_{\text{epoxide}}$ distances for the pair of epoxide vicinal protons are in good agreement with those obtained experimentally via the above ENDOR measurements. This comparison reinforces the assertion that the changes observed in the ENDOR spectra are due to the inherent chirality in the complex forcing the chiral epoxide molecules to adopt different binding conformations.

In the HKR,⁵ and related $[\text{CrCl}(\mathbf{1})]$ catalysts,⁸ the active species bear an anionic π -basic donor group trans to the bound epoxide, similar to the current $[\text{VO}(\mathbf{1})]$ model. A recent mechanistic study^{5b} indicates that the key step in enantiodiscrimination in the HKR of epoxides by $[\text{Co}(\mathbf{1})(\text{X})]$ species (X = anion) is the interaction of the activated nucleophile $[\text{Co}(\mathbf{1})(\text{H}_2\text{O})(\text{OH})]$ and the activated epoxide complex $[\text{Co}(\mathbf{1})(\text{OH})(\text{epoxide})]$ and *not* the enantioselective binding of epoxide substrates by $[\text{Co}(\mathbf{1})(\text{X})]$ species. The current ENDOR study supports this by showing that chiral Lewis acids such as $[\text{VO}(\mathbf{1})]$ bind the “mismatched” epoxide more strongly. If this mismatched species were involved in the hydrolysis step, the opposite enantiomers would be observed as products. The implication of these results is that although, for example, the (R,R) - $[\text{Co}(\mathbf{1})(\text{OH})]$ + (R) -**5** complex is likely to have a higher formation constant than (R,R) - $[\text{Co}(\mathbf{1})(\text{OH})]$ + (S) -**5**, it is the more rapid reaction of the latter complex with $[\text{Co}(\mathbf{1})(\text{H}_2\text{O})(\text{OH})]$ that determines the stereochemical outcome.

Acknowledgment. We acknowledge EPSRC funding for the ENDOR Centre (GR/R17980/01) and postgraduate support for R.R. Strevens (GR/L80447/01) and R.J. Tucker. We also acknowledge the EPSRC national mass spectrometry service (Swansea).

Supporting Information Available: Figures 1 and 2 and corresponding EPR/ENDOR spectra (PDF). This material is available free of charge via the Internet at <http://pubs.acs.org>.

References

- (1) For an excellent historical overview, see: Mason, S. F. *Molecular Optical Activity and the Chiral Discriminations*; Cambridge University Press: Cambridge, 1980.
- (2) For a recent relevant example, see: Bobb, R.; Alhakimi, G.; Studnicki, L.; Lough, A.; Chin, J. J. *J. Am. Chem. Soc.* **2002**, *124*, 4544.
- (3) (a) Murphy, D. M.; Fallis, I. A.; Farley, R. D.; Tucker, R. J.; Avery, K. L.; Willock, D. J. *Phys. Chem. Chem. Phys.* **2002**, *4*, 4937. (b) Tucker, R. J.; Fallis, I. A.; Farley, R. D.; Murphy, D. M.; Willock, D. J. *Chem. Phys. Lett.* **2003**, *380*, 757.
- (4) (a) Rirst, G. H.; Hyde, J. S. *J. Phys. Chem.* **1970**, *52*, 4633. (b) Hoffman, B. M.; Martinsen, J.; Venters, R. A. *J. Magn. Reson.* **1984**, *59*, 110. (c) Hurst, G. C.; Henderson, T. A.; Kreilick, R. W. *J. Am. Chem. Soc.* **1985**, *107*, 7294. (d) Hoffman, B. M. *Proc. Natl. Acad. Sci. U.S.A.* **2003**, *100*, 3575. (e) Smoukov, S. K.; Kopp, D. A.; Valentine, A. M.; Davydov, R.; Lippard, S. J.; Hoffman, B. M. *J. Am. Chem. Soc.* **2002**, *124*, 2657. (f) Bolm, C.; Martin, M.; Gescheidt, G.; Palivan, C.; Neshchadin, D.; Bertagnolli, H.; Feth, M.; Schweiger, A.; Mitrikas, G.; Harmer, J. *J. Am. Chem. Soc.* **2003**, *125*, 6222. (g) Schweiger, A.; Jeschke, G. *Principles of Pulse Electron Paramagnetic Resonance*; Oxford University Press: New York, 2001.
- (5) (a) Tokunaga, M.; Larrow, J. F.; Kakiuchi, F.; Jacobsen, E. N. *Science* **1997**, *277*, 936. (b) Nielsen, L. P. C.; Stevenson, C. P.; Blackmond, D. G.; Jacobsen, E. N. *J. Am. Chem. Soc.* **2004**, *126*, 1360.
- (6) (a) Attanasio, D. *J. Phys. Chem.* **1986**, *90*, 4952. (b) Schweiger, A.; *Structure and Bonding*; Springer: Berlin, 1982; Vol. 51, p 1.
- (7) See Supporting Information for details of the computational work.
- (8) Hansen, K. B.; Leighton, J. L.; Jacobsen, E. N. *J. Am. Chem. Soc.* **1996**, *118*, 10924.

JA045491S